JOURNAL OF MATERIALS SCIENCE 20 (1985) 1889–1900

R-curve behaviour of metallic glass ribbons

W. HENNING, M. CALVO*, F. OSTERSTOCK*
Institute für Werkstoffkunde und Werkstofftechnik, Technische Universität Clausthal, D-3392 Clausthal-Zellerfeld, West Germany

In this paper we show that metallic glass ribbons obey the laws of plane stress fracture very well. The centre crack tensile specimen was used to investigate the subcritical crack extension prior to catastrophic failure on two alloys. The resulting R-curves are used to reconstruct the experimentally observed variation of the critical stress intensity factor, K_c, with initial crack length. Taking into account only the measured subcritical crack extension (up to 50 μm) a good qualitative correlation is obtained. Starting from that experimental observation and using very simple assumptions about the variation of the shape of the R-curve as the material embrittles, we propose a schematic description of how K_c may vary when the ribbons are annealed and if short or large initial crack lengths are used. An experimental verification is made on one of the alloys.

1. Introduction

It is well established that metallic glass ribbons in the as-quenched state fracture mostly by plane stress crack propagation. Fracture occurs by shear at an angle of about 45° to the tensile axis. The plane stress state was confirmed by examination of the development of the plastic zone ahead of the loaded crack. It was shown that the Dudgale [1] or Bilby–Cottrell–Swinden [2] models describe the behaviour of these materials very well [3, 4]. They have thus been classified as elastic, perfectly plastic materials.

If a notched specimen is not thick enough for plane strain conditions the crack propagates in a pure plane stress or even a mixed state. The critical stress intensity factor is then called K_C rather than K_{Ic}. The measured value of K_c depends on two geometrical factors. The first is the specimen thickness. This determines the relative amounts of slant and square fracture. The second factor is the initial crack length, a_0. This is linked to subcritical crack growth during loading and is described as R-curve behaviour. This phenomenon and its effects have been theoretically investigated [5, 6] and the practice of plotting R-curves has already been developed and published [7]. The observation that K_c depends on initial crack length has not yet been seen in metallic glass ribbons. However, this point is important as toughness measurements are carried out using various methods, i.e. either the centre cracked tensile panel (CCT) or the so-called fatigue-up-to-rupture method. In the latter case an unnotched specimen is loaded in fatigue and the critical crack length is measured after rupture. If K_C depends on initial crack length, two main consequences are to be expected. First, if the toughness of a given material is measured using the same specimen type, its value will depend on the experimental facilities of the laboratory, such as laser drilling, spark erosion with wires or foils. Secondly, this first effect is enhanced if an attempt is made to measure the variation in toughness; the shape of the R-curves is changed, hence the variation of K_c with initial crack length changes too. A corollary may be fatigue lifetime measurements where both effects are combined.

The aim of this paper is to look initially for experimental evidence of a dependence of the measured K_c values on crack length. Following this some R-curves will be plotted and used to reconstruct theoretically the expected change of

*Permanent address: Equipe Matériaux-Microstructure du LA 251, ISMRa – Université, F-14032 Caen Cedex, France.

0022–2461/85 $03.00 + .12

the K_c values with crack length. Their influence on the toughness measurements and the deviation from the Bilby–Cottrell–Swinden (BCS) model will finally be discussed.

2. Materials and experimental procedure

Two alloys have been investigated: alloy A, a $Fe_{40}Ni_{40}B_{20}$, 40 μm thick and 2.3 mm wide ribbon from Vakuumschmelze, and alloy B, a $Co_{70.43}Cr_{21}W_{4.5}B_{2.4}Si_{1.6}C_{0.07}$, 50 μm thick and 25 mm wide ribbon from Allied-Chemical.

To measure K_c, the CCT specimen was used. A full section of alloy A was used while alloy B was divided in two to get a specimen width of about 12 mm with polished edges. Specimen total lengths were 70 to 80 mm with a gauge length of 50 mm. The critical value of the stress intensity factor, K_c was calculated using:

$$K_c = \sigma_r Y(\pi a)^{1/2} \quad (1)$$

where: σ_r is the rupture stress; a is the half-crack length at the onset of rapid crack propagation. It was measured, for each specimen in an Hitachi scanning electron microscope, which was also used for the fractographic investigations; Y is the crack length dependent geometrical correction factor. We used a polynomial expression computed by ISIDA [17]

$$Y = 1 + 0.128\,(a/b) - 0.288\,(a/b)^2 + 1.525\,(a/b)^3 \quad (2)$$

Spark erosion, with low power ($V < 50$ V and $I <$ 0.1 A) and 20 μm thick copper foils, was used to get centre notches with relative length, $2a_0/2b$, ranging from 0.05 to 0.8. Initially, these notches had been extended by fatigue to avoid any influence of insufficient sharpness and of the eventually heat affected zone.

Special attention was paid to the loading arrangement as shown in Fig. 1. The specimen ends were fixed between two steel plates using a jig. Effects of residual non-alignment were reduced by allowing the steel plates to rotate in a fork holder which was in turn fixed in the grips of a 1121 or 1185 Instron testing machine. Breaking of the specimen at the edge of the steel plates was avoided by protecting the specimen ends with a piece of the metglass ribbon affixed to them with silver or copper paint. This design proved effective since only very few specimens, even unnotched, broke in the fixture grips and then only at the beginning of the investigation, due to mishandling.

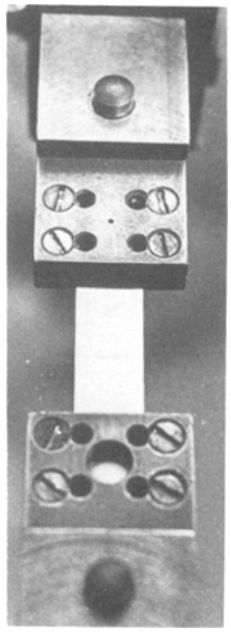

Figure 1 Experimental set-up with notched specimen.

To record the subcritical crack growth the following procedure was used. Sets of specimens having the same initial crack length were stressed to different levels, the crack front was then marked by fatigue cycling and the specimen finally loaded up to rupture. After this the stable crack extension was measured in the scanning electron microscope, SEM. Optical measurements on the surface proved unsuccessful and misleading because of the presence of the plastic zone. Compliance measurements were not possible since no precise load displacement recording was to be expected.

3. Results

3.1. Evidence of R-curve behaviour

3.1.1. Background

R-curves describe the increasing resistance a material exhibits against the propagation of a crack as the latter is stressed. During loading a crack of initial length, a_0, grows in a stable manner to some extent, which is related to the resistance the material offers via the development of the plastic zone. If the material's resistance is plotted in terms of stress intensity, K_R, as a function of the stable crack extension, Δa, one obtains an R-curve similar to that shown by the thick full curve in Fig. 2. The R-curve is believed to depend only on specimen thickness and material properties. The point of instability, i.e. K_C, is defined

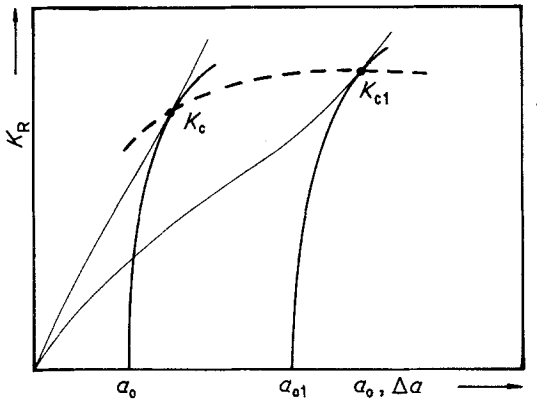

Figure 2 Schematic illustration of R-curve and the resulting effect on the influence of initial crack length, a_0, on K_C.

by the following conditions:

$$K_c = K_R \tag{3}$$

and

$$\delta K_c/\delta a > \delta K_R/\delta a \tag{4}$$

where K is stress intensity applied on the crack via loading. Graphically, as shown in Fig. 2, it is the point of tangency between the loading curve (thin curve) and the K_R-curve. If a specimen with a larger initial crack length is loaded, the K_R-curve is simply shifted and another point of instability K_{c1} is obtained which is different from the previous K_C. Continuing this procedure with longer or shorter cracks, results in the dotted curve in Fig. 2, which denotes the dependence of K_c on the initial crack length and is denoted as R-curve behaviour. Further details are given by Brown and Strawley [5] and Schwalbe [6].

3.1.2. Alloy A

The results with fatigue extended notches are shown in Fig. 3. The expected effect, as schematically depicted in Fig. 2, is clearly obtained. The relative crack length, $2a_0/2b$, is varied from 0.1 to 0.7. The highest K_C value is 44 MPa $m^{1/2}$ ($2a_0/2b = 0.25$) whereas lower ones (about 30 MPa $m^{1/2}$) are measured for a relative crack length of 0.1. These values have been measured on specimens which were not stiffened. Crack and specimen buckling may thus occur due to compressive stresses which act through the specimen width [9]. Buckling was avoided by using teflon platelets as shown in Fig. 4. The resulting effect on K_C is shown in Fig. 5. The values from stiffened specimens (full circles) are compared with those from Fig. 3 (open circles). The influence of stiffening becomes noticeable at relative crack lengths higher than 0.2. When the crack length range was extended, the R-curve effect was more emphasized, and K_C values higher than 50 MPa $m^{1/2}$ ($0.25 < 2a_0/2b < 0.45$) or smaller than 25 MPa $m^{1/2}$ ($2a_0/2b < 0.05$) were reached. The smoothed maximum which exists explains why Freed *et al.* [10] did not observe this effect although they used the CCT specimen for aluminium alloys. Their relative crack length varied from 0.15 to 0.5. However, our results are in contrast with those of Waku and Masumoto [3] who used relative crack lengths between 0.02 and 0.16.

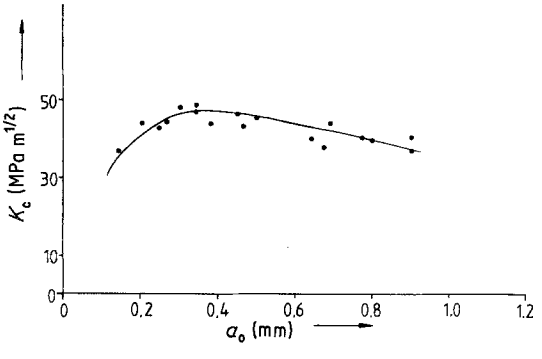

Figure 3 Experimental evidence of the influence of a_0 on K_C for alloy A (as-quenched) with fatigue extended notches.

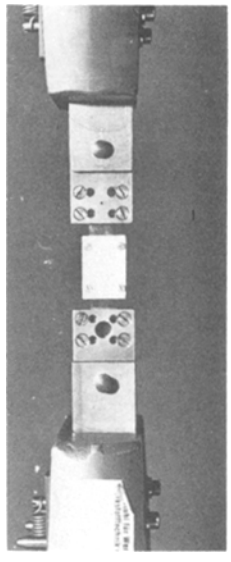

Figure 4 Experimental set-up with stiffened specimens using Teflon platelets.

Initially, we expected the spark erosion technique to locally heat the specimen and partly relax the glassy structure in the vicinity of the

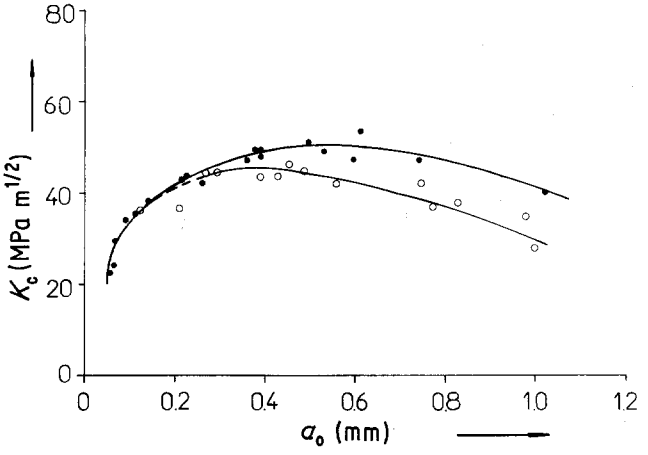

Figure 5 Effect of specimen stiffening on the crack length dependence of K_C, for as-quenched alloy A. • with Teflon, ○ without Teflon.

notch root. To verify this effect another set of measurements was made using as-eroded notches (without stiffening platelets). Results are shown in Fig. 6; full points are from fatigue extended notches and open points from as-eroded ones. The two sets of values can be fitted by the same curve. This is due either to the narrowness of the heat affected zone which is crossed by subcritical crack extension, or to an excessive size which would not be overlapped, even by the fatigue crack (50 μm–100 μm). The former case is correct since no discontinuity on the fractographic pattern was observed.

3.1.3. Alloy B

As previously noted the width of these specimens was only half that of the as-quenched ribbon. The results (K_C as a function of relative crack length) are reported in Fig. 7. Initially, they are rather disturbing. The values, independent of crack length, are scattered between 20 and 77 MPa m$^{1/2}$. SEM fractographic investigation on each specimen was necessary to classify them. This was done on the basis of the commonly defined vein and chevron patterns. Initially the vein pattern had been related to plane stress conditions and the chevron pattern to plain strain conditions because they were associated with respectively high and low K_C values. As a matter of fact, careful observation of the fracture surface with a chevron pattern [11–13] shows that on the side of the specimen, a surface inclined 45° to the tensile axis and decorated with veins exists. On the other hand, the annealed specimens (500 K) in Fig. 16 all had a chevron pattern, but if plane strain conditions had been achieved the thick and the thin full lines should have the same value at least after some annealing time. It is not the case, some doubt is thus cast on the assumption that chevron pattern defines ideal plane strain conditions. Keeping this in mind, we have nevertheless used the vein and chevron patterns to classify the results of Fig. 7. This is possible because the specimens all had the same thickness and the scatter is crack-length independent. Some specimens had an essentially pure and regular vein pattern on a fracture surface inclined 45° to the tensile axis (Fig. 8a). These all had higher K_C values and are located in the upper hatched area of Fig. 7, exhibiting the expected crack length dependence. Others had a well defined chevron pattern (Fig. 8c) and are located in the lower hatched area; for these an approximate toughness value of 20 MPa m$^{1/2}$ is obtained which is independent of crack length. In considering this value care should however be taken because the chevron patterns were not equally rough and the scatter may mask a dependence on crack length. The samples may

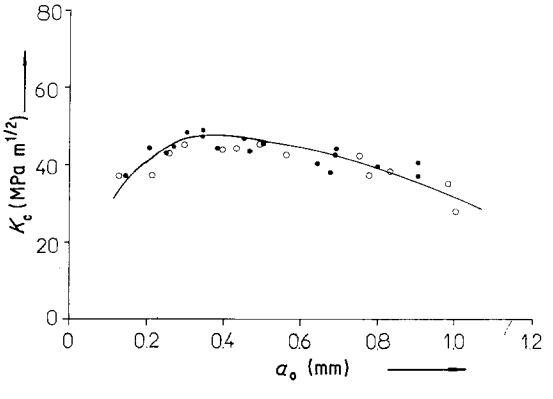

Figure 6 Comparison of K_C values obtained either with as-eroded (○) or fatigue extended (•) notches. As-quenched alloy A.

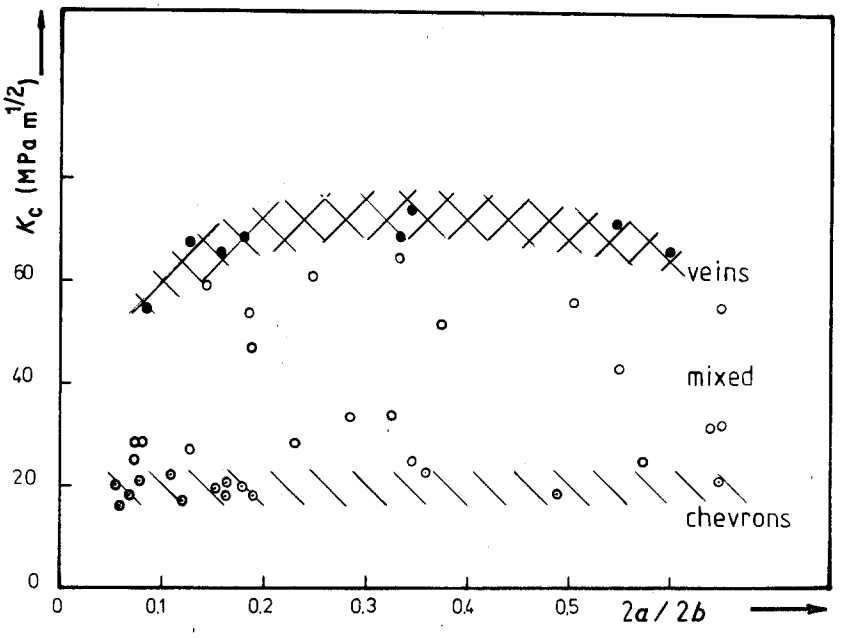

Figure 7 Results obtained with alloy B. They have been classified on the basis of the fractographs of Fig. 8. Full circles are with vein pattern and, dotted circles with chevron pattern; open circles are from mixed features.

thus not have the same relaxed state but we did not make a second attempt to classify the points with low K_C values.

All the other specimens had mixed fractures (Fig. 8b). They lie between the two hatched areas of Fig. 7. An accurate ordering of these intermediate values proved to be difficult since the crack may start to propagate with either a chevron or vein pattern. The three fractographic features mentioned above are shown in Fig. 8. This scatter reveals that metallic glass ribbons may be quite inhomogeneous. The fact that whole sections of the specimens may be more or less relaxed is surprising. The technical reasons which

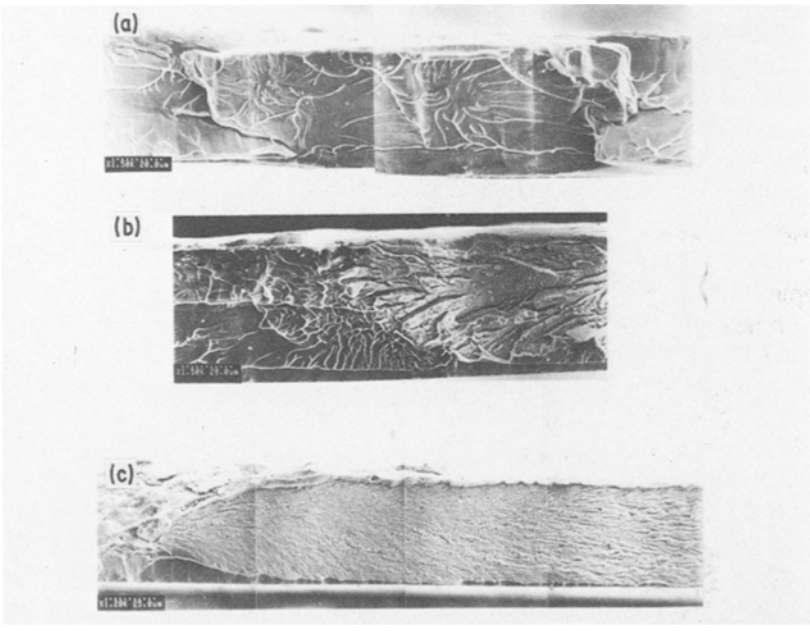

Figure 8 Fractographs of alloy B. (a) A typical vein pattern, (b) mixed chevron and vein pattern, (c) chevron pattern.

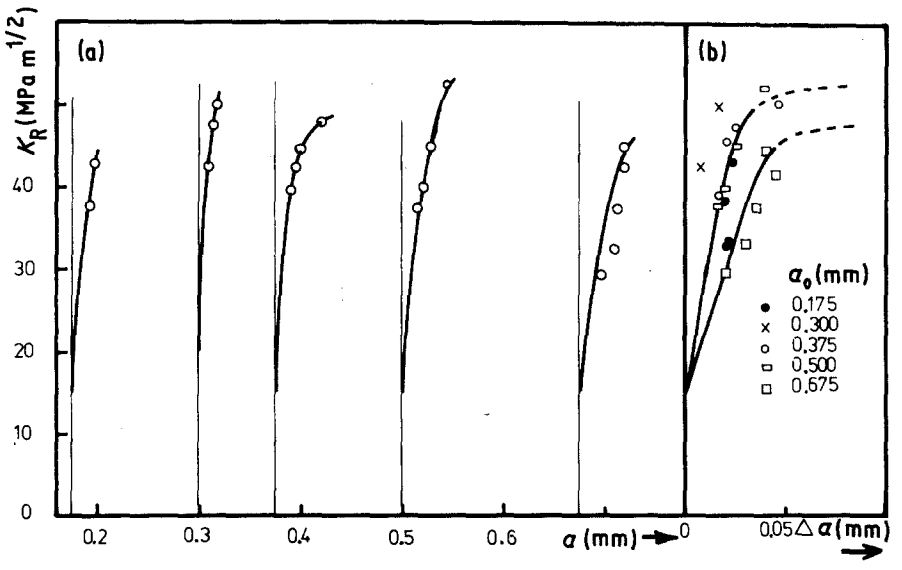

Figure 9 (a) R-curves obtained with various initial curve length. Each point results from one specimen. (b) Plot of all experimental values in an unique K_R against Δa plot.

permit such an "as-quenched" state were not investigated, but it is of important since one considers the influence on mechanical or corrosion properties. Separate investigations [18] on the same ribbon using a Guinier camera and metallographic procedure indicated that this material was partly crystallized, but with respect to our results, the crystallization is inhomogeneous too.

3.2. Plotting of R-curves

Owing to the time consuming procedure and the previously noted inhomogeneities of alloy B, the extent of subcritical crack extension was determined only on alloy A. Sets of specimens having the same initial crack length were used. All the measurements were made using the teflon platelets as buckling inhibitors. The results, as a plot of K (applied stress intensity factor) against Δa (crack extension), are shown for each initial crack length in Fig. 9a. The stress intensity factor, K, was used as a coordinate instead of the strain energy release rate, G. Subcritical crack extension up to 45 μm are recorded. Theoretically, R-curves are expected to be independent of initial crack length but influenced by probe-thickness. The plot of Fig. 9b, which gathers all the subcritical crack extension values in an unique Δa against K scheme hardly confirms this. Whereas the experimental points for the short cracks show the same trend, large Δa values for a given K-level, have been measured with the longer cracks and some of the shorter. Whether it is due to inhomogeneities or is normal scatter is not yet clear. Thus, both curves have been used to construct the theoretical K_C against a_0 dependence which will be shown in the following. Fig. 10 is a fractographic view of the subcritical crack extension. It is a well defined fractographic feature, and at first the crack extends in plain strain conditions. As soon as rapid failure begins there is a change towards plane stress conditions; the failure surface is inclined 45° to the tensile axis and has a vein pattern.

3.3. Construction of the K_C against crack length dependence

Using the experimental results of Fig. 9 the crack length dependence of K_C has been reconstructed following the procedure outlined in Section 3.1. The result is shown in Fig. 11. The evolution of K with increasing crack length for some values of the applied stress, σ, has been calculated (thin curves). Then, french curves representing the crack resistance were made from the data in Fig. 9b and their tangential contact points with the K-curve found by sliding the french curves along the abscissa axis (crack length). Two major problems arose during this procedure. Firstly, for the medium and larger crack lengths experimental data for the R-curve were missing in the higher K values range. This was extrapolated using a parabolic type curve from the experimental data

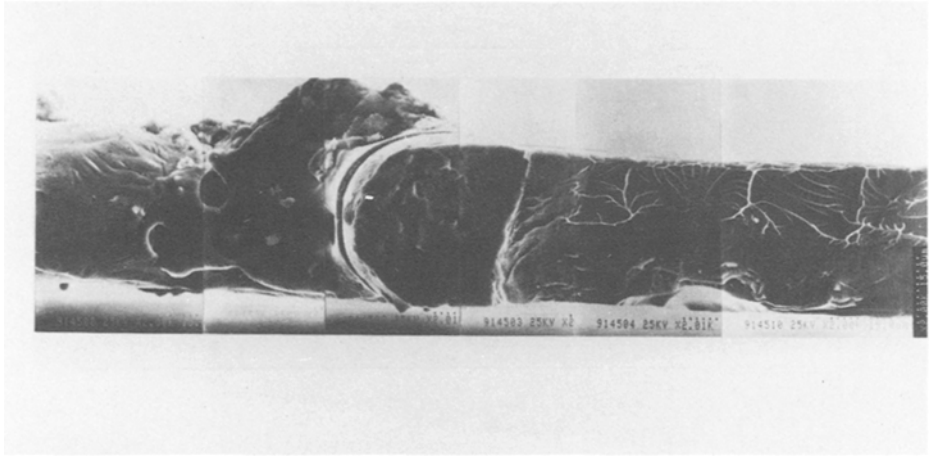

Figure 10 Fractographic view of subcritical crack growth from an as-eroded specimen.

as shown by the broken lines in Fig. 9b. The extrapolation is correlated by measurement on other specimens whose initial cracks are between those of the four sets used here (Fig. 5). Secondly, two main curves had been obtained (Fig. 9b), and the question arose as to which curve to use. Since medium and large crack lengths each exhibited a consistent behaviour, we used the experimental value obtained in each crack length range. For the shorter cracks we used both, to look for the resulting effect. This can be seen in Fig. 11. The broken lines shows the measured evolution of the K_C values. The calculated evolution is described by the full line which is divided in two for the shorter crack lengths. The lowest K_C values were obtained with the R-curve for the longest crack. The effect of how the R-curve was chosen is quite significant. Even if the experimental and calculated K_C against a curves are not exactly superposed they show the same shape and the R-curve behaviour can be considered to have been experimentally verified.

A more accurate construction of the K_C against a dependence is excluded because the scatter in the experimental data is too large. This scatter and thus inaccuracy of the R-curve may be due to the inhomogeneous relaxation state of the metallic glasses. Even the $Ni_{40}Fe_{40}B_{20}$ ribbon suffered from this lack of homogeneity as could be shown, during the fracture toughness measurements of temperature embrittlement either by annealing or during liquid nitrogen temperature measurements [8, 12]. For example, for annealing time less than 100 min the scatter is high and may be compared qualitatively to those of alloy B [12, 13].

4. Discussion

The R-curve behaviour of metallic glass ribbons has been verified. One may now discuss its effect

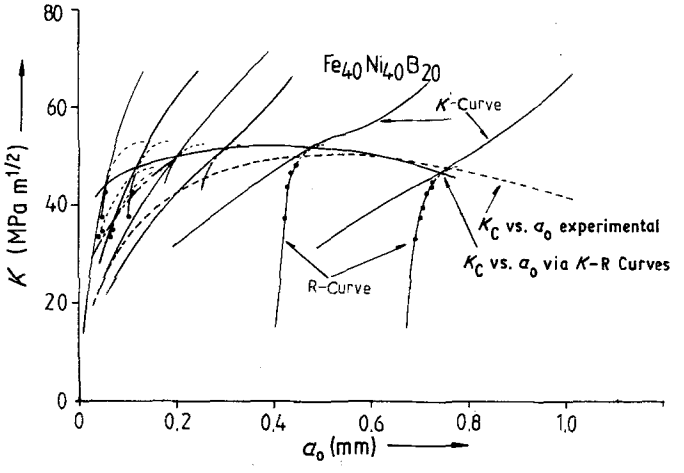

Figure 11 Reconstruction of K_C against a_0 dependence using the experimental R-curves. The result is shown as the full and dotted line. The measured dependence is shown by the broken line.

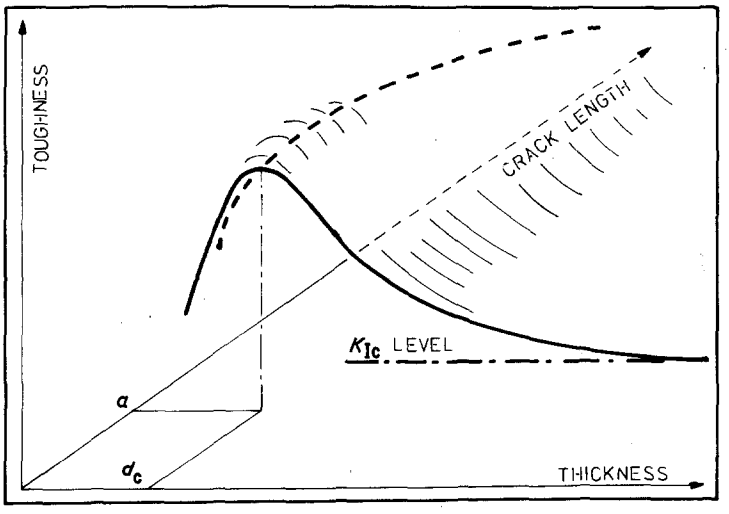

Figure 12 Schematic representation of the dependence of the toughness (K_C) on crack length, a, and specimen thickness.

on the temperature embrittlement measurements using various methods or crack lengths. This must be done within the framework of fracture mechanics and is shown schematically in Fig. 12. It represents a surface in a three dimensional reference system. Abscissae are specimen thickness, d, and initial crack length, a_0. The ordinates are the measured K_C values. As long as plane strain conditions are not achieved K_C is a function of two variables, a_0 and d. The influence of d, which should always be investigated at a constant and defined a_0, has been verified on metallic glass ribbons by Davies [15] and Hunger [14]. They first annealed some samples, secondly they polished them down to various thicknesses and finally measured the fracture toughness K_C. As theoretically expected, K_C increased as the thickness decreased. Unfortunately fractographic observations were not made simultaneously. These results as well as those reported in this paper show that metallic glasses obey the laws of fracture mechanics well.

The influence of a_0, which was the target of this work is depicted by the dashed curve in Fig. 12. Its amplitudes depends on the shape of the R-curve. We will now speculate how the amplitude and shape of the resulting K_C against a_0 curve at constant d may vary when the shape of the R-curve varies as the material embrittles. If at constant thickness, samples are embrittled, the change in shape of the R-curve is expected to evolve as schematically depicted in Fig. 13. For highly plastic materials the R-curve may look like the left hand side in Fig. 13, where high K (or G) values are reached. On the other hand for very brittle materials, the right hand curve may be representative. We assume that metallic glass ribbons vary from the first to the others as the material is embrittled during annealing. As a material is embrittled the change of the shape of the R-curve will induce a change in the K_C against a_0 behaviour as depicted in Fig. 14. If one plots the K_C against brittleness variation for various initial crack lengths the scheme in Fig. 15 is obtained. The scheme in Fig. 15 may be understood as cuts at constant d of Fig. 80 in the work of Schwalbe [6]. One only needs to consider that, as a material becomes more brittle, the value of d_C decreases. In order to verify this, a comparison was made with some results of Hunger [14]. Hunger used the fatigue-up-to-rupture method to measure the annealing embrittlement of a $Ni_{40}Fe_{40}B_{20}$ alloy. Unnotched samples were annealed and then fatigue cycled up to rupture. After some time, the

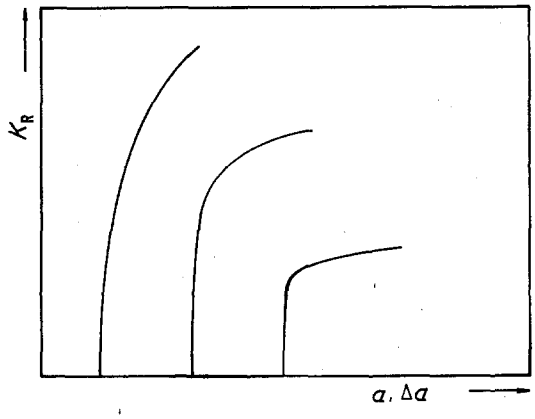

Figure 13 Schematic representation of the change in shape of R-curves as the material is embrittled.

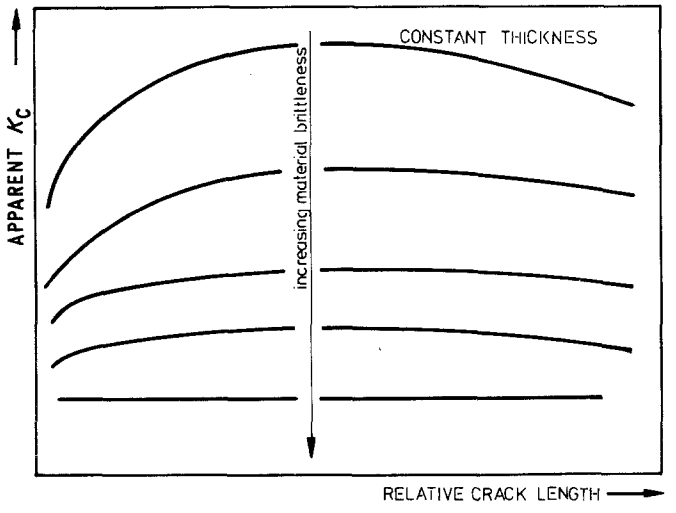

Figure 14 Schematic representation of the change in the R-curve behaviour as the material is embrittled. It can be regarded as cuts, at increasing thickness, in the surface of Fig. 12.

specimen broke from the edge and the fatigue crack length was measured. The maximum applied stress and crack length were then used to calculate K_C. The critical fatigue crack lengths were short, so the K_C values may be ranged in the hatched area of Fig. 15. We have used the same ribbon and annealing conditions at 500 K as Hunger and notched CCT-samples ($2a_0/2b \cong 0.4$). The results are plotted in Fig. 16. The thin lines represent the results of Hunger and the full thick line describes our results. A very good qualitative fit with Fig. 15 is obtained. Furthermore, the results obtained with the CCT-panel are smoothed like the hardness measurements.

The previously published results from fracture mechanics measurements on metallic glass ribbons do not exhibit such a pronounced R-curve effect. The reason is that various states of relaxation may be obtained if one combines composition, quenching temperature and rate, and specimen thickness. A first example has already been shown in the lower hatched area of Fig. 7. A second one is shown in Fig. 17; the material used is a $Ni_{81}P_{19}$ alloy, 38 μm thick [13]. Although the scatter is larger than in alloy A it has not reached the extent which was observed with alloy B. Generally speaking, as the ribbons become thicker, the state of relaxation is more pronounced and thus the R-curves are better described by the right hand side of Fig. 13. The effects of initial crack length on K_C are thus smoothed. However, the influence of the resulting cooling inhomogeneities on mechanical bearing capacities, especially at very low temperatures, needs further investigation.

As already mentioned, some authors have shown that the development of the plastic zone

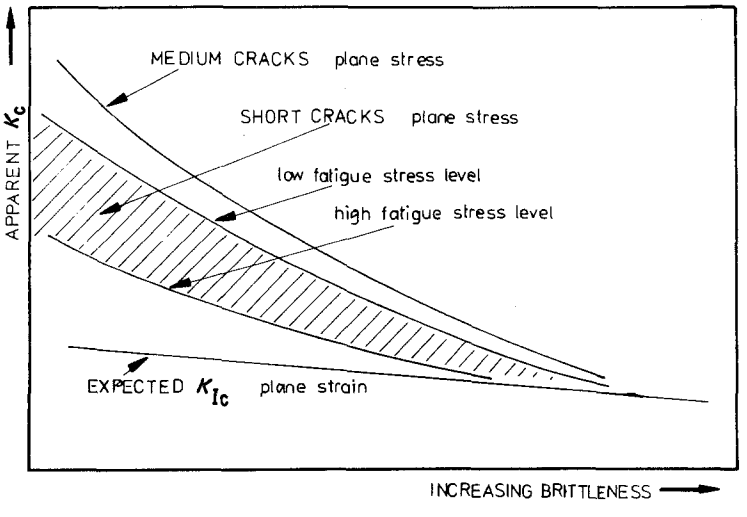

Figure 15 Schematic representation of the various expected evolutions of K_C as the material is embrittled.

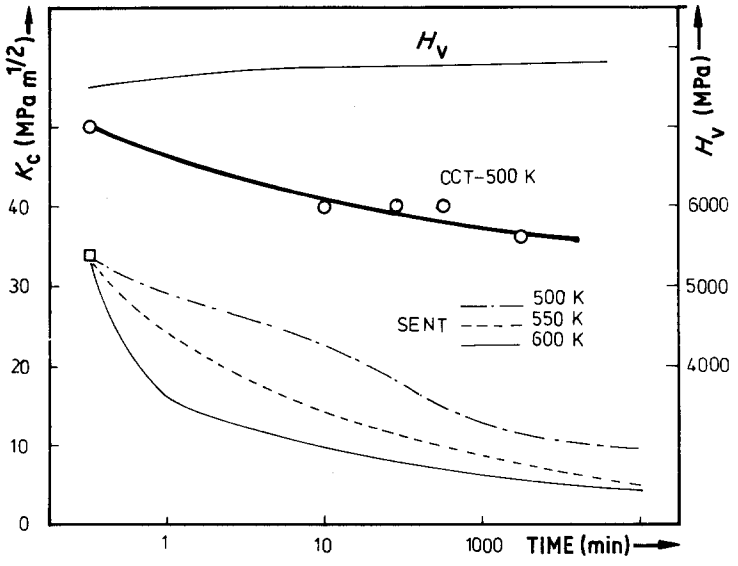

Figure 16 Experimental verification of Fig. 15 using a $Ni_{40}Fe_{40}B_{20}$ alloy (25 μm × 2.35 mm).

ahead of the loaded crack is very well described by the BCS model [1–4]. We have also checked this model with alloy A. Fatigue extended notches were used. Hence the increase in size of the plastic zone could be measured only for stresses higher than half the fracture stress. Incremental loading was used and the length of the slip lines was taken as a measure of the plastic zone, Z_p. We also calculated the theoretical size using:

$$Z_p = a_0 \left(\sec \frac{\pi \sigma_a}{2 \sigma_y} - 1\right) \qquad (5)$$

where:
a_0 is the initial crack length (eroded + fatigue), σ_a is the applied stress, and σ_y is the yield stress of the material. A value of 3200 MPa gave the best fit. It is in accordance with the microhardness value, of H_v, about 11000 MPa. The critical crack opening displacement (*COD*) was also calculated using the following relationship:

$$COD_{crit} = \frac{8 \sigma_r a_0}{\pi E} \ln \sec \frac{\pi \sigma_r}{2 \sigma_y} \qquad (6)$$

where: σ_r is the stress at rupture and E is the Young's modulus. Measurements with strain gauges gave a value of $E = 1.4 \times 10^5$ MPa which fits well in the plot of Whang *et al.* [16]. The values of COD_{crit} are between 4 and 6 μm in accordance with those published by Waku and Masumoto [3] for a $Ni_{78}Si_{10}B_{12}$ alloy.

The calculated and measured values of the size of the plastic zone are compared in Fig. 18. For low stress levels ($\sigma_a < 0.7\ \sigma_r$) the fit is good, but for higher ones the calculated values are

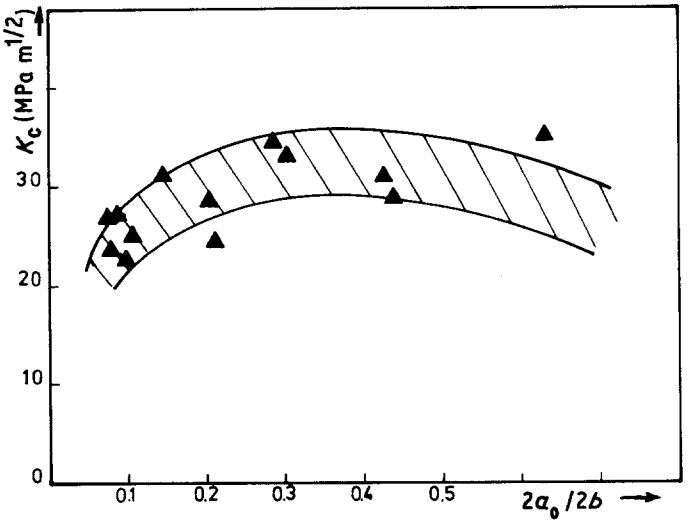

Figure 17 Dependence of K_C on initial crack length for an as-quenched $Ni_{81}P_{19}$ alloy, 40 μm thick. Ribbon thickness is 38 μm.

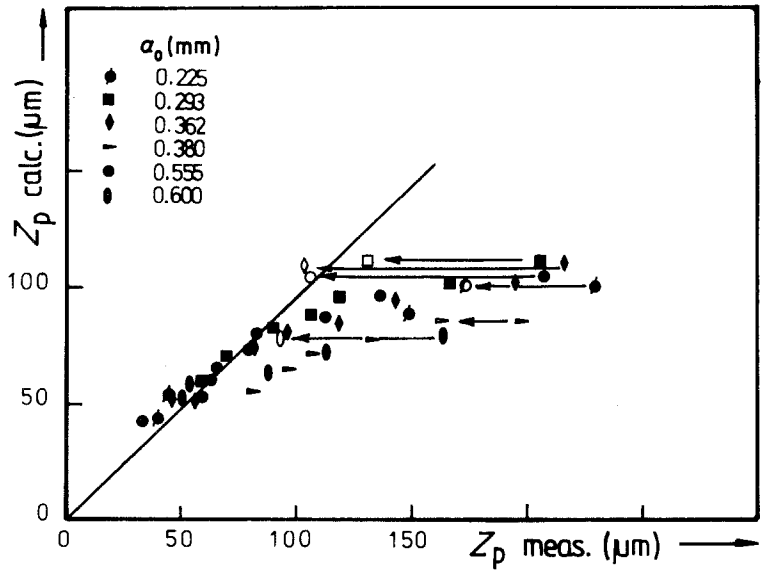

Figure 18 Comparison of the measured and calculated size of the plastic zone for alloy A. The arrows show the extend of subcritical crack growth. All specimens, except the one with $a_0 = 0.380$ mm, are fitted very well by a value of σ_y of 3200 MPa.

smaller than the measured ones. This departure from the ideal behaviour begins at stress levels where subcritical crack growth was measurable (see Fig. 9). After rupture, the extent of subcritical crack extension has been deduced from the measured Z_p values. The resulting values are the open points which are in accordance with calculated values. This means that the subcritical crack extension is accompanied by a shift of the plastic zone. This is normal since the crack resistance curve is determined by the development of the plastic zone.

5. Conclusion

The expected dependence of K_C on the initial crack length (defined as R-curve behaviour) has been verified on metallic glass ribbons. The strength of this effect, depends on the state of relaxation of amorphous structure. Thus, it may not be measurable on some alloys. If it exists, it strongly affects the measurement of the material embrittlement during annealing and has disastrous effects on the load bearing capacities either at room or low temperatures or on fatigue lifetimes.

An interesting question which arose during this work is whether a chevron pattern is really an indication of plane strain conditions. This point needs further investigation.

Acknowledgements

This work was done while F. Osterstock was at Technische Universität Clausthal as an Alexander von Humboldt fellow and M. Calvo was supported at the same University by DAAD (German Service for University Exchanges).

References

1. D. S. DUGDALE, *J. Mech. Phys. Solids* 8 (1960) 100.
2. B. A. BILBY, A. H. COTTRELL and K. H. SWINDEN, *Proc. R. Soc.* **A272** (1963) 304.
3. Y. WAKU and T. MASUMOTO, Proceedings of the 4th International Conference on Rapidly Quenched Metals, Sendai 1981, pp. 1395–8.
4. S. KOBAYASHI and S. M. OHR, *ibid.* pp. 1353–6.
5. W. F. BROWN and J. E. STRAWLEY, ASTM STP 381, (American Society for Testing and Materials, Philadelphia 1964).
6. K. H. SCHWALBE, "Bruchmechanik metallischer Werkstoffe", edited by C. HANSER (München, 1980).
7. Recommended practice ASTM E561 76T, ASTM–STP–632 American Society for Testing and Materials, Philadelphia 1977) pp. 241–59.
8. W. HENNING, F. OSTERSTOCK, B. L. NORDIKE, Annual Meeting of DGM (German Society of Metallurgy), Erlangen, May 1983.
9. J. R. DIXON and J. S. STRANNIGAN, "Fracture 1969", Plenum Press, (Brighton, England, 1966) pp. 105–18.
10. C. N. FREED, A. M. SULLIVAN and J. STOOP, ASTM STP 514 (American Society for Testing and Materials, Philadelphia, 1972) pp. 98–113.
11. S. HENDERSON, J. V. WOOD and G. W. WEIDMANN, *J. Mater. Sci. Lett.* **2** 373 (1983).
12. W. HENNING, Diplomarbeit, June 1983, Technishce Universität Calusthal, Clausthal-Zellerfeld, West Germany (1983).
13. M. CALVO, DEA, October 1983, University of Caen, France.
14. G. HUNGER, PhD thesis, Technische Universität

Clausthal, Clausthal-Zellerfeld, West Germany (1983).
15. L. A. DAVIES, *J. Mater. Sci.* **10** (1975) 1557.
16. S. H. WHANG, D. E. POLK and B. C. GIESSEN, Proceedings of the 4th International Conference on Rapdily Quenched Metals, Sendai 1981, pp. 1365–7.
17. M. ISIDA, *Eng. Fract. Mech.* 7 (1975) 505.
18. H. W. BERGMANN, Habilitationsschrift, 1983, Technische Universität Clausthal, Clausthal-Zellerfeld, FRG.

Received 6 February
and accepted 21 June 1984